# Optical Absorption by Impurities in $p$-Type Gallium Phosphide

J. M. Dishman and M. DiDomenico, Jr.
*Bell Telephone Laboratories, Murray Hill, New Jersey* 07974
(Received 5 April 1971)

We present the results of a detailed study of optical absorption due to the oxygen donor and the Zn-O and Cd-O nearest-neighbor impurity complexes in $p$-GaP. In solution-grown crystals doped for optimum luminescence efficiency we find that the absorption coefficient below the band gap over the visible region (1.7 eV $< h\nu <$ 2.3 eV) is typically in the range 2–4 $cm^{-1}$. Although a major fraction of the absorption in this region results from the O and the Zn-O or Cd-O centers, we find that other inadvertent impurities (e.g., Si, Cu, S, and C) also contribute to the absorption. The temperature dependence of the individual absorption bands due to Zn-O and Cd-O are found to be well described by a semiclassical single-linear-mode model for phonon-coupled impurity absorption. In contrast, the highly skewed oxygen absorption band requires (on theoretical grounds) a hybridization of the standard configuration-coordinate approach with a model which takes into account the continuum nature of the initial (valence band) state of the free-to-bound absorption. Qualitative agreement is found between the hybridized model and the shape of the oxygen band. Because of the large degree of lattice coupling associated with the oxygen transitions, we find that the oscillator strength in absorption is a factor 4–12 times stronger than that in emission. This effect is attributed to differences in the lattice configuration depending on whether the oxygen donor is in a neutral or ionized state. For the Zn-O transitions, a factor-of-3 enhancement of absorption to emission is found.

## I. INTRODUCTION

Although the intrinsic absorption edge[1–4] and the extrinsic infrared free-carrier absorption[5–7] of $n$- and $p$-type GaP have been extensively studied, the absorption spectrum below the indirect band edge (2.26 eV at 300 °K) in the range 1.0 eV $< h\nu <$ 2.3 eV has received little attention. For luminescence applications the absorption coefficient in this region is extremely important since it determines how much of the internally generated light escapes from the high index of refraction material.[8] In this paper we present a detailed study, through luminescence excitation and transmission measurements, of several prominent impurity absorption bands related to the presence of oxygen in $p$-GaP. We report the existence of a new band (at ~ 7300 Å at 300 °K) due to the photoneutralization of the deep (~ 900 meV) substitutional unpaired oxygen donor. In addition, we present data on the absorption spectrum (at ~ 5800 Å) associated with the presence of Zn-O nearest-neighbor impurity complexes, as well as the absorption spectrum (at ~ 6200 Å) resulting from Cd-O complexes. Even in the absence of intentional doping with oxygen, it has been found that oxygen is inevitably incorporated into $p$-GaP during growth.[9] Thus, we expect the oxygen-related absorption bands to be dominant components of the total absorption coefficient in the range 1.0 eV $< h\nu <$ 2.3 eV in all $p$-type material. In our transmission study of crystals grown from Ga solution we find additional components of absorption which we attribute to the inadvertent presence of impurities such as S, Si, C, and Cu. We present evidence to show that these inadvertent impurities produce absorption tails, both on the low-energy side of the band edge and on the high-energy side of the free-carrier absorption spectrum.

A major problem in understanding the shape of the oxygen absorption band relates to the fact that the electronic states of the oxygen donor are very strongly coupled to the lattice.[10–12] As a result, the usual theories of band-to-impurity absorption in semiconductors,[13–15] which neglect phonon interactions, cannot be applied. We show, however, that the oxygen absorption band can be described qualitatively by combining the usual band-to-impurity model with the configuration-coordinate approach[16,17] commonly used to describe impurity absorption of color centers in I-VII compounds. This hybridized model predicts that the usual Gaussian-like absorption spectrum will be distorted or skewed toward higher energies as observed experimentally.

The large degree of phonon cooperation (lattice relaxation) associated with optical transitions at the deep oxygen donor also influences the relative strengths of the dipole matrix elements for absorption and emission. We find, for samples whose oxygen concentration is known from a previous determination,[8] that the oscillator strength for optical absorption by ionized oxygen donors is 4–12 times larger than the oscillator strength for the inverse process of emission from the neutralized donors. For Zn-O nearest-neighbor complexes we find that the absorption oscillator strength is three times stronger than the emission oscillator strength.

Because of their isoelectronic character, ab-

sorption at Cd-O and Zn-O centers is dominated by exciton effects.[18–20] In contrast to the band-to-impurity oxygen donor absorption, both the initial and final states in absorption at the isoelectronic complexes can be treated as discrete, and the conventional configuration-coordinate model can be applied directly. We find, for example, that the widths of the absorption bands vary as $\coth(\hbar\omega/kT)$, as predicted by the semiclassical model.[16] Using a single-linear-mode coupling model, this behavior allows us to relate the position of the maxima of the bands to their no-phonon energies. The no-phonon energies in turn give us the temperature dependence of the electron binding energies of the Cd-O and Zn-O complexes. We find that the Cd-O binding energy is reduced from 0.40 to 0.36 eV as the temperature is increased from 10 to 300 °K. Over the same temperature range we find that the Zn-O binding energy is reduced from 0.26 to 0.22 eV, which is in agreement with other independent results.[8,21]

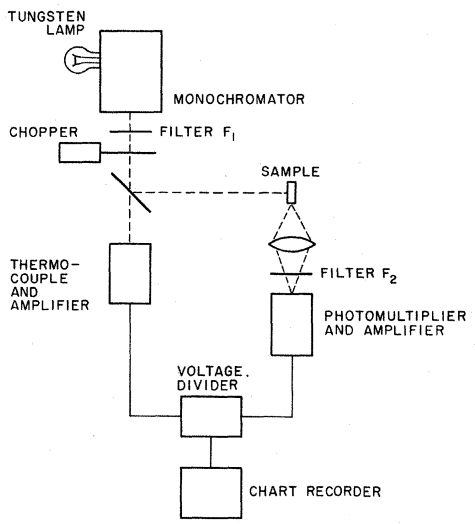


FIG. 1. Schematic diagram of apparatus used for photoluminescence excitation measurements. See text for details.

## II. EXPERIMENTAL

In order to study optical impurity absorption in $p$-GaP over the temperature range 1.8–400 °K, two types of experimental methods were employed. In the first, photoluminescence excitation spectra were recorded in order to study the individual shapes of the absorption bands due to the O donor, and the Cd-O and Zn-O nearest-neighbor impurity complexes. The second method consisted of conventional transmission measurements on GaP platelets in the spectral range $0.4\ \text{eV} < h\nu < 2.4\ \text{eV}$. Transmission data were obtained (to temperatures of 20 °K) using a dual-beam spectrophotometer modified for use with a liquid-helium cryostat. Transmission experiments detect not only the oxygen-related impurity absorption, but also absorption connected with shallower impurities which do not emit efficient luminescence at room temperature because of thermalization effects.

A schematic diagram of the apparatus used in the luminescence excitation experiments is shown in Fig. 1. In Zn, O- and Cd, O-doped $p$-GaP, red photoluminescence was excited with monochromatic light ($\lambda < 630\ \text{m}\mu$). The red emission was due to radiative recombination at Zn-O, and Cd-O complexes. In addition, infrared luminescence was generated as a result of recombination at isolated oxygen donors. These emission bands were separated by an appropriate choice of filters $F_1$ and $F_2$. In order to eliminate scattered light from the monochromator, filter $F_1$ was selected to pass only wavelengths shorter than those in the luminescent band of interest. For determination of the oxygen absorption band, filter $F_1$ consisted of a 1-59 CS Corning filter together with a long-wave-pass interference filter cutting off at 400 m$\mu$ (to prevent second-order effects). Filter $F_2$ was a polished slice of GaAs, whose band gap corresponds approximately to the low-energy threshold of the oxygen band. In determining the Cd-O and Zn-O absorption bands, filter $F_1$ was a combination of interference filters having a pass band from 400 to 650 m$\mu$, while $F_2$ was composed of Corning CS 5-44 and CS 2-64 filters together with a 750-m$\mu$ short-wave-pass interference filter (the latter to block out oxygen luminescence). When the infrared emission from oxygen was sampled, an S-1 photomultiplier was used as a detector. For the red emission an S-20 photomultiplier was used. In order to normalize out the spectral variations of the tungsten lamp and the monochromator grating, a portion of the incident beam was sampled by a thermocouple detector and its output was divided into the response of the luminescence detector. The thermocouple was found to have a flat response to within 20% over the wavelength range of interest. Because the luminescent output was low from the samples studied at room temperature, the maximum slit width of the monochromator was used, limiting the resolution of the excitation spectra to about 6 meV.

The absorption spectra of a series of Zn, O-doped solution-grown crystals were obtained as a function of temperature for $0.4\ \text{eV} < h\nu < 2.3\ \text{eV}$ from transmission measurements on thin platelets. The absorption coefficients $\alpha$ were calculated from

$$t = (1-R)^2/(e^{\alpha d} - R^2 e^{-\alpha d}), \qquad (1)$$

where $t$ is the transmission ratio, $d \sim 0.25$–$0.5$ mm is the crystal thickness, and $R$ is the reflection coefficient determined from published indexes of re-

fraction data.[5,22] All transmission samples were polished with 0.1-$\mu$ diamond paste on {111} faces and cleaned with trichloro-ethylene solvent. It has been our experience that polishing with 0.1-$\mu$ diamond paste does not introduce measurable surface loss. Polishing with larger-grain-size diamond paste not only results in substantial surface loss but also significantly distorts the shape of the absorption spectrum by introducing a long tail on the band edge which extends, in some cases, to $h\nu \approx 1.4$ eV.

The crystals chosen for study were grown from Ga solution[23] in sealed quartz tubes and were free from gross imperfections over selected areas. Of the five crystals studied, one was undoped and the remaining four were double doped with 0.02 mole% $Ga_2O_3$ and 0, 0.007, 0.07, and 0.15 mole% Zn in the melt. Since oxygen is poorly controlled in GaP and there is evidence[9] that heated quartz ampoules can introduce oxygen, we believe that all five crystals contained oxygen as a dopant at a level of the order of $10^{17}$ cm$^{-3}$.[8] All crystals, including the undoped, were $p$ type. The net acceptor concentrations of our crystals were[24] $2\times10^{17}$, $10^{18}$, and $2\times10^{18}$ cm$^{-3}$ for crystals with 0.007, 0.07, and 0.15 mole% Zn added to the melt.

## III. OXYGEN-RELATED IMPURITY ABSORPTION

Oxygen, substituting for phosphorus in the GaP lattice, is a deep donor, binding electrons at 4 °K with an energy of 895 meV.[10,11] In $p$-type material the major optical absorption process due to unpaired oxygen is expected to be photoneutralization of ionized oxygen donors through the elevation of electrons from the valence band. The spectral shape and temperature dependence of this photoneutralization process and its related emission band will be discussed in detail in this section.

It is well known that during crystal growth the Coulomb attraction between ionized donor and acceptor atoms can result in large fractions of the impurity atoms associating in the form of nearest-neighbor pairs.[25,26] In gallium phosphide, nearest-neighbor Zn-O and Cd-O impurity complexes have been shown to be the source of the efficient red luminescence commonly utilized in GaP light-emitting diodes.[18–20] Recombination at these complexes is considerably more complicated than for the two-state oxygen donor, since they are, in effect, isoelectronic centers for which three recombination states must be considered.[8,27] In an unexcited $p$-type crystal these complexes are neutral and unoccupied by electrons or holes. Under photoexcitation, the complexes may become occupied by a single electron giving rise to a negatively charged state, or they may be occupied by both an electron and hole, giving rise to a neutral bound-exciton state. Thus, in a $p$-type crystal we expect optical impurity absorption due to acceptor-oxygen complexes to arise from two sources: (a) photoionization of the complex by promotion of an electron from the valence band, and (b) direct photocreation of excitons bound to the complex. The spectral region in which these processes take place depends on the electron binding energy of the complex which, to a first approximation, is just the binding energy of the isolated oxygen donor reduced by the Coulomb repulsion between the electron and the negatively charged nearest-neighbor acceptor. The latter energy is 549 meV (using a nearest-neighbor distance of 2.36 Å), so that at low temperature the binding energy of the complex is expected to be $\approx$350 meV, independent of the acceptor binding energy. The measured *exciton* binding energy (at 20 °K) of the Cd-O complex is 421 meV.[18-20] Using an inferred hole binding energy of 35 meV,[19] one finds that the electron binding energy of the Cd-O complex is 386 meV,[19] which is in reasonable agreement with the expected value. An exciton binding energy for the Zn-O complex has not been measured (no sharp exciton no-phonon line has been observed), but calculations presented here indicate that the electron binding energy is about 260 meV. The energy positions of the O, Cd-O, and Zn-O centers are summarized in Fig. 2.

The extremely large chemical shift of the oxygen donor binding energy (the effective-mass binding energy in GaP is 45 meV)[28] indicates that the donor electron is very localized in the central cell surrounding the impurity. Hence, we expect that the local strain field associated with the lattice polarization due to the ionized oxygen donor will change drastically as the donor undergoes a transition from the ionized to the neutral state. These large changes in local strain imply that most of the os-

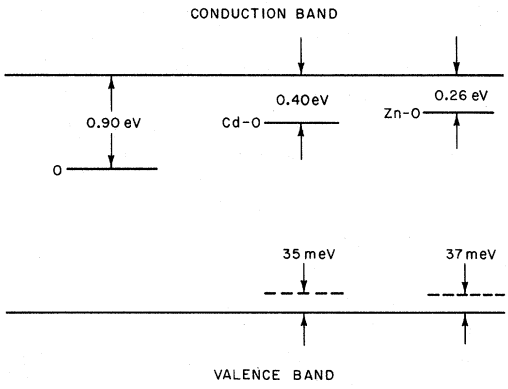


FIG. 2. Schematic energy level diagram for GaP (at 0 °K) showing energy levels in the forbidden gap associated with the oxygen donor and the Cd-O and Zn-O isoelectronic complexes. Solid and dashed lines indicate the energy levels of bound electrons and holes, respectively.

cillator strength of the photoneutralization absorption at oxygen is associated with the dissipation of strain energy (lattice relaxation) to various phonon modes of the lattice. Thus, we expect to be able to apply the semiclassical configuration-coordinate model[16] in which the effects of lattice coupling are emphasized. However, in this model the continuum nature of the initial (valence band) states of the system is not taken into account. We show that this effect can be taken into account in the formulas for the energy dependence of the absorption coefficient in a simple way, so that the resulting expressions for the absorption spectrum are a straightforward combination of the configuration-coordinate model and the no-phonon effective-mass-like models for band-to-impurity absorption.

Since the effective electron binding energies of the Zn-O and Cd-O isoelectronic complexes also show large chemical shifts (associated with the chemical shift of the oxygen component), we expect strong lattice coupling to be present in optical transitions involving the tightly bound electron at these centers. Because excitonic transitions dominate the optical spectra associated with these complexes,[18–20] they are somewhat more suitable than the oxygen donor for analysis by the standard semiclassical model[16] in which discrete energy values are assumed for both initial and final states. We find that the temperature dependence of the width of the Zn-O and Cd-O absorption bands can be fitted to a model with simple linear-mode coupling to the lattice. This allows us to relate the shift in the peak position of the absorption band to the reduction in electron binding energy of the centers with increasing temperature.

### A. Isolated Oxygen Donor

The temperature dependence of the isolated (unpaired) oxygen donor absorption spectrum obtained from a sample grown from Ga solution containing 0.007 mole% Zn and 0.02 mole% $Ga_2O_3$ is shown in Fig. 3. The spectra were determined from the intensity of the excited photoluminescence below 1.435 eV (i.e., filter $F_2$ in Fig. 1 passed only photons with energy less than this value). Only the structure below ~2.3 eV is due to optical absorption at the ionized oxygen donor. The structure at $C$ is due to the photocreation of excitons bound to nitrogen isoelectronic centers, which are inadvertently present in the solution-grown crystals used. These bound excitons can excite the oxygen luminescence either through tunneling of the trapped electron to an oxygen center, or by thermalization of the exciton off of the nitrogen center and subsequent recapture of the minority carrier at the ionized oxygen donor. For photon energies above the band gap (denoted by $D$ in Fig. 3), the oxygen luminescence is excited by direct capture of the photogenerated minority carriers. Figure 3 shows that the efficiency of the above gap (at $D$), relative to the below gap (at $B$), excited oxygen luminescence is a rapidly varying function of temperature. This variation is related to the thermalization of other dominant recombination centers in the crystal which capture minority carriers in competition with the oxygen centers, and will be discussed elsewhere.[29]

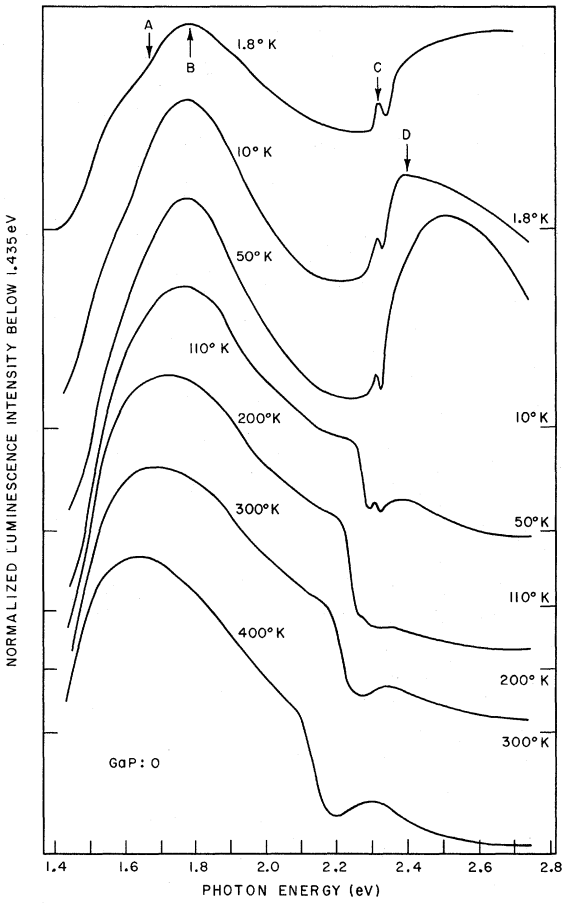


FIG. 3. Photoluminescence excitation spectra of the ionized oxygen donor at several temperatures obtained by monitoring the infrared emission from neutral oxygen below 1.435 eV. The zero levels of the spectra have been shifted for clarity and are denoted by fiducial marks along the ordinate axes. The structure at $A$, $B$, $C$, and $D$ is discussed in the text.

The oxygen absorption band centered at ≈1.8 eV is very broad (>0.8 eV) and non-Gaussian. At low temperatures on the low-energy side of the spectrum ($A$ in Fig. 3) a change in slope is noted whose origin is unknown. At all temperatures a very long high-energy tail is observed extending up to and beyond the band-gap energy. As the temperature is increased, the peak of the band shifts to lower energies and the band shape becomes more skewed toward the high-energy side. Above 110 °K the

half-power point on the high-energy side is at an energy greater than the band-gap energy and can no longer be observed. In order to compare with theoretical models of impurity absorption, one wishes to know the second moment of the spectrum as a function of temperature. Because most of the high-energy tail is obscured by above band-edge absorption, a meaningful plot of the second moment cannot be obtained for the oxygen absorption band.

A comparison of the absorption and emission bands due to isolated oxygen in $p$-GaP is shown in Fig. 4. Below 60 °K the dominant photoemission from neutral oxygen results from radiative donor-acceptor pair recombination in which an electron on a neutral oxygen donor recombines with a hole on a distant neutral acceptor[11] (e.g., zinc, as is the case in Fig. 4). The 60 °K emission spectrum in Fig. 4 results from O-Zn pair emission and its phonon replicas[12] (five replicas of the no-phonon pair band can be made out in the original data shown in Fig. 1 of Ref. 12). At 90 °K and above, the pair emission is replaced by free-to-bound emission.[12] In this process a free hole is captured by the neutral oxygen donor, thereby ionizing it. This radiative transition is the inverse of the photoneutralization process which produces the 1.8-eV absorption band. (In the 90 °K emission spectrum of Fig. 4 the no-phonon line of the free-to-bound emission, as well as two replicas, are resolvable in the original data shown in Fig. 1 of Ref. 12.)

The theoretical description of the oxygen photoneutralization absorption spectrum is complicated by two effects. The first is the considerable phonon cooperation associated with the optical transitions, and the second is the continuum of valence band levels associated with the initial ground state. The standard theories of optical impurity absorption in direct-gap semiconductors containing effective-mass impurities (for example, the Eagles[13] or Dumke[14] hydrogenic models or the more recent quantum-defect model of Bebb[15]) cannot be immediately applied to photoneutralization of oxygen in GaP, because of both the indirect character of the band gap and the central-cell character of the oxygen donor wave function. Both of these effects contribute to the phonon cooperation associated with the photoneutralization transition. On the other hand, the configuration-coordinate approach,[16] used where coupling to the lattice is strong, is always formulated in terms of discrete energy levels for both the ground and excited states. It is a straightforward matter, however, to modify the usual formalism in order to take into account the continuum nature of the initial state in the oxygen photoneutralization problem. When this is done we find that the photoneutralization spectrum for an impurity tightly coupled to the lattice can be thought of as being made up of a set of weighted

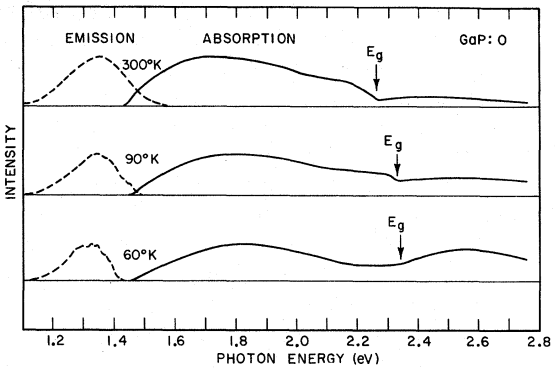


FIG. 4. Comparison of emission and absorption bands due to the oxygen donor in $p$-GaP. Arrows denote position of band-gap energy at each temperature. Absorption spectra are from luminescence excitation data as in Fig. 3. Emission spectra are from Ref. 12, and at lower temperatures show discrete structure due to phonon replication.

phonon replicas of the usual effective-mass optical impurity absorption spectrum (e.g., Dumke, Eagles, and Bebb). In this way the oxygen photoneutralization spectrum represents a hybrid of the configuration-coordinate and effective-mass-like models of impurity absorption.

Following Fowler and Dexter[17] we can express the photoneutralization cross section at photon energy $E$ for transitions from the electronic state $a$ to the electronic state $b$ as

$$\sigma_{ab}(E)=\left(\frac{\xi_{eff}(E_{ab})}{\xi_0}\right)^2 \frac{E_{ab}}{n(E_{ab})}\,\frac{4\pi e^2}{3\hbar c}\,|M_{ab}|^2\,\frac{S_{ab}(E)}{2J_a+1}\,. \tag{2}$$

In this equation $\xi_{eff}$ is the effective field at the impurity center, $\xi_0$ is the average field in the medium, $n$ is the index of refraction, $M_{ab}$ is the electronic dipole matrix element, $J_a$ is the angular momentum quantum number of the lower state, $E_{ab}$ is the energy difference between the two electronic states, and $S_{ab}(E)$ is the shape of the absorption spectrum due to phonon cooperation. If we make use of the Condon approximation and assume that $M_{ab}$ is independent of the lattice coordinates, the shape function can be written in the form[16,30]

$$S_{ab}(E)=\langle\textstyle\sum_\beta |\langle a\alpha|b\beta\rangle|^2\,\delta(E_{b\beta}-E_{a\alpha}-E)\rangle_{\rm av}\,. \tag{3}$$

In Eq. (3), $\langle a\alpha|$ and $|b\beta\rangle$ are the vibrational wave functions for the lower and upper electronic states, respectively, and $E_{a\alpha}$ and $E_{b\beta}$ are their energy eigenvalues. The notation $\langle\rangle_{\rm av}$ represents a thermal average over the initial $\alpha$ vibrational states (associated with the electronic state $a$) and the sum extends over all final $\beta$ vibrational states (associated with the electronic state $b$). For convenience, we will neglect the dependence of $\xi_{eff}$ and $n$ on $E_{ab}$. In

Sec. V we will consider the effect of the lattice configuration on the matrix elements for absorption $M_{ab}$ and emission $M_{ba}$, i.e., when the Condon approximation breaks down and $M_{ab} > M_{ba}$. In usual treatments[30] of impurity absorption involving phonon cooperation, the spectral shape is entirely determined by Eq. (3) and consists of a set of weighted $\delta$ functions representing the emission and absorption of phonons concomitant with the electronic transition. In the semiclassical approximation generally discussed, this shape is approximately Gaussian. For the photoneutralization process considered here, the state $a$ is one of a continuum of valence band states. The total photoneutralization cross section is a sum over all such states, weighted by a density of states factor:

$$\sigma_b(E) = \sum_a g_a \sigma_{ab}(E) . \quad (4)$$

To evaluate Eq. (4) we replace the sum by an integral over the kinetic energy $E_v$ of a hole in the valence band. The energy $E_{ab}$ can be written as $E_{ab} = E_0 + E_v$, where $E_0$ is the energy difference between the impurity level and the top of the valence band. In the photoneutralization and photo-ionization models, which neglect phonon cooperation,[13-15] the matrix element $M_{ab}$ is evaluated between Bloch band states and effective-mass impurity states made up from Bloch functions. As a result, $|M_{ab}|^2$ is energy dependent. Taking $|M_{ab}|^2 \propto S(E_v)$, where $S(E_v)$ is a shape function, and using Eqs. (2)–(4) we find that the photoneutralization cross section $\sigma_b(E)$ for transitions between the valence band and the electronic impurity state $b$ is given by

$$\sigma_b(E) = B \int dE_v g_a(E_v)(E_O + E_v)\, S(E_v) \times \langle \sum_\beta |\langle a\alpha | b\beta\rangle|^2 \delta(E_{b\beta} - E_{a\alpha} - E)\rangle_{av} , \quad (5)$$

where $B$ is a constant. If the impurity interacts with a single-lattice mode of energy $\hbar\omega$, then[30]

$$E_{b\beta} - E_{a\alpha} = E_O + E_v + (\beta - \alpha)\hbar\omega . \quad (6)$$

Making use of Eq. (6) and taking the sum outside the integral in Eq. (5), we obtain, through evaluation of the $\delta$ function,

$$\sigma_b(E) = \langle \sum_\beta B |\langle a\alpha | b\beta\rangle|^2 g_a[E - E_O - (\beta - \alpha)\hbar\omega] \times [E - (\beta - \alpha)\hbar\omega]\, S[E - E_O - (\beta - \alpha)\hbar\omega]\rangle_{av} . \quad (7)$$

If we assume that $g_a(E_v) \propto E_v^{1/2}$, then

$$\sigma_b(E) = \langle \sum_\beta B' |\langle a\alpha | b\beta\rangle|^2 [E - E_O - (\beta - \alpha)\hbar\omega]^{1/2} \times [E - (\beta - \alpha)\hbar\omega]\, S[E - E_O - (\beta - \alpha)\hbar\omega]\rangle_{av} , \quad (8)$$

where $B'$ is a constant. The photoneutralization spectrum described by Eq. (8) is similar in appearance to the spectrum of Eqs. (2) and (3) with the $\delta$ functions replaced by an effective shape factor

$$S_{eff}(E) \equiv [E - E_O - (\beta - \alpha)\hbar\omega]^{1/2} [E - (\beta - \alpha)\hbar\omega] \times S[E - E_O - (\beta - \alpha)\hbar\omega] . \quad (9)$$

We show schematically in Fig. 5 the difference between the optical absorption for two discrete levels [Eq. (3)], and that where the initial state is a continuum of levels [Eq. (8)]. We continue the assumption that the coupling with the lattice involves only a single linear mode of energy $\hbar\omega$, and furthermore assume $T = 0$ °K so that $\alpha = 0$. The bars in Fig. 5 represent the weighted $\delta$ functions of Eq. (3), assuming a semiclassical model in which the weighting factors result in a Gaussian shape. For comparison, the dashed curves show two of the terms ($\beta = 3$ and 6) in Eq. (8). Because of the long high-energy tails, the result of replacing the $\delta$ functions with the shape factors $S_{eff}(E)$ is to shift the peak of the original Gaussian to higher energies and to greatly skew the absorption band toward higher energies.

Although the interaction of the oxygen donor in GaP with the lattice undoubtedly involves several modes, quadratic as well as linear, we expect the basic features of the spectra in Fig. 3 to be explained in a qualitative manner by Eq. (8). The spacing between replicas in Fig. 5 has been chosen relative to the width of the $S_{eff}(E)$ curves in order to approximate the expected situation for oxygen in GaP, viz., $\hbar\omega \approx 50$ meV. The effective shape $S_{eff}(E)$ was determined from the Bebb model[15] with a quantum defect of zero, characteristic of a very deep donor.

### B. Cadmium-Oxygen Impurity Complex

The Cd-O luminescence excitation spectra obtained at various temperatures from a crystal grown from gallium solution doped with 10 mole% Cd and 0.02 mole% $Ga_2O_3$ is shown in Fig. 6. In obtaining these spectra, the red luminescence between 1.82 and 1.44 eV resulting from radiative recombination at Cd-O nearest-neighbor complexes was monitored (through proper choice of filter $F_2$ in Fig. 1) as a function of the exciting photon energy from the monochromator. As was the case in Fig. 3, structure attributable to absorption at inadvertent nitrogen impurities was observed (at $B$ in Fig. 6) about 10 meV below the band edge over the temperature interval from 45 to 180 °K. The shape of the maxima at $C$ results from surface recombination which dominates at short incident wavelengths. In analogy with the oxygen luminescence excitation spectra (Fig. 3), the temperature dependence of this peak is more rapid than the temperature dependence of the below gap excited luminescence maximum at $A$.

The absorption band due to Cd-O is non-Gaussian

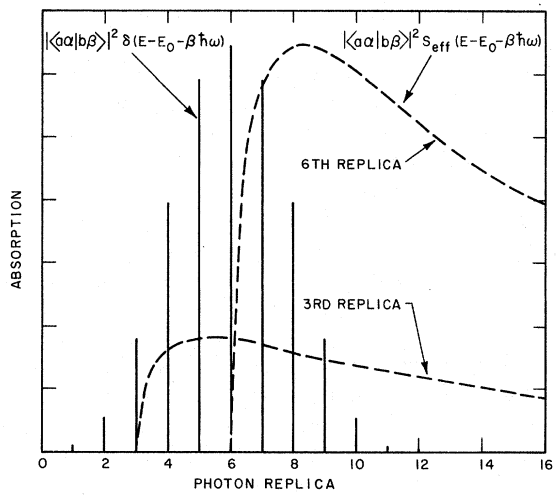


FIG. 5. Schematic comparison of impurity absorption bands computed for two different initial electronic states. Solid lines show semiclassical band shape consisting of a $\delta$ function for each phonon replica weighted by a Gaussian envelope, assuming a discrete initial electronic state [Eq. (3)]. Dashed curves illustrate (for the third and sixth replica) how each $\delta$ function is replaced by a broad shape function [Eq. (9)] when absorption results from a continuum of band states [Eq. (8)].

with a long high-energy tail which extends to photon energies well above the band gap energy. In describing the temperature dependence of this band it is useful to define an effective width $W = 2(E_{ab} - E_{1/2})$, where $E_{ab}$ is the photon energy at the maximum of the band and $E_{1/2}$ is the photon energy corresponding to the half-power point on the low-energy side of the peak. (The actual half-width of the band cannot be measured at all temperatures because the high-energy half-power point is obscured by absorption at the band edge.) The temperature dependence of $W$ for the Cd-O absorption band is plotted in Fig. 7. The data are well described by the usual semiclassical model in which the impurity is strongly coupled to a single linear vibrational mode of the lattice, i.e., $W$ is constant at low temperature and varies as $T^{1/2}$ at higher temperatures. Using the nomenclature of Keil, [30] this model predicts an approximately Gaussian absorption band whose width is given by

$$W_A = 2a\hbar\omega\,[0.693\,\coth(\hbar\omega/2kT)]^{1/2}\,, \qquad (10)$$

where $\hbar\omega$ is the energy of the lattice mode and $a$ is a dimensionless constant proportional to the strength of the coupling between the impurity and the lattice. The solid curve in Fig. 7 represents a fit of Eq. (10) to the data using $\hbar\omega = 29.9$ meV.

The single-linear-mode theory leading to Eq. (10) assumes that both initial and final electronic states are discrete. Previous discussions of Cd-O absorption[18,20] have, in fact, assumed a discrete initial electronic state, and have considered only processes of the form

$$h\nu \rightarrow E_g - E_x + n\hbar\omega\,, \qquad (11)$$

i.e., the absorbed photon creates an exciton bound by an energy $E_x$ plus $n$ phonons of energy $\hbar\omega$ ($E_g$ is the band-gap energy). In addition to this process, we expect another process

$$h\nu - E_v \rightarrow E_g - E_t + n\hbar\omega, \qquad (12)$$

in which an electron from a depth $E_v$ in the valence band is excited into a negatively charged bound state of the Cd-O complex (binding energy $E_t$), along with the emission of $n$ phonons. The process described by Eq. (12) is analogous to the photoneutralization process discussed previously for the oxygen donor [see Eq. (8)]. There are two reasons why we expect the process described by Eq. (11) to

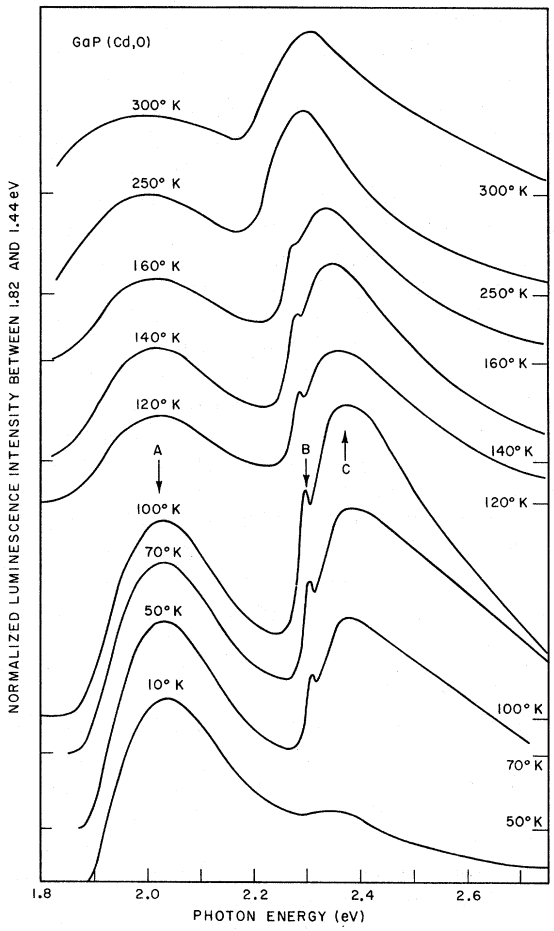


FIG. 6. Photoluminescence excitation spectra of the neutral Cd-O impurity complex at several temperatures obtained by monitoring the red emission from the photoexcited complex in the range 1.82–1.44 eV. The zero levels have been shifted as in Fig. 3. Structure at $A$, $B$, and $C$ is discussed in the text.

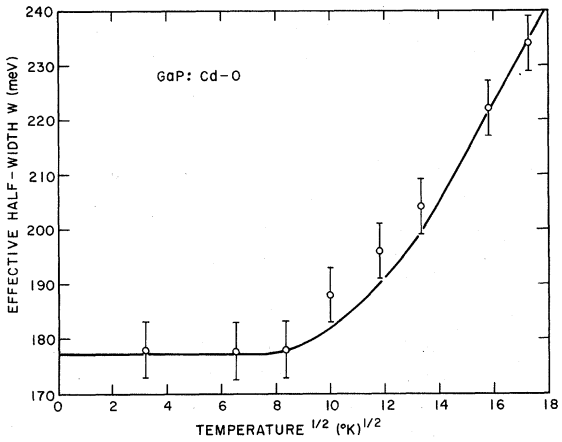


FIG. 7. Effective half-width $W$ (defined in text) for the Cd-O absorption band as a function of the square root of temperature. Solid curve is fit of Eq. (10) to the data obtained by taking $\hbar\omega = 29.9$ meV.

dominate over that of Eq. (12). First, we have found that the single-mode model adequately describes the temperature dependence of $W$ [Eq. (10) and Fig. 7]. It seems unlikely that the absorption band due to photo-ionization of the Cd-O centers [described by expressions of the form of Eq. (8)] would have the simple temperature dependence given by Eq. (10). Indeed, in contrast to the prediction of Eq. (10) and Fig. 7 we find, for the oxygen-donor absorption band, that the effective width $W$ *decreases* with increasing temperature. Second, other investigators[18,20] have observed sharp-line structure connected with the Cd-O band, attributable to direct photocreation of bound excitons. This structure is not as pronounced in absorption as in emission, but nevertheless, it suggests a dominant role for the process of Eq. (11).

The single-linear-mode theory[30] predicts a simple relationship between the no-phonon energy $E_{np}$ [$\alpha = \beta$ in Eq. (3)] and the peak absorption energy $E_{ab}$, viz.,

$$E_{np} = E_{ab} - \tfrac{1}{2}\alpha^2\hbar\omega. \tag{13}$$

If the Cd-O absorption is dominated by excitonic transitions, then Eq. (13) can be used to deduce the binding energy of the exciton through the identification $E_x = E_g - E_{np}$. In Fig. 8 we plot this binding energy versus temperature, where we have used the known no-phonon energy at 10 °K ($E_{np} = 1.908$ eV)[18,20] to determine the constant $\alpha = 3.05$ from Eq. (13). If we assume that the binding energy $E_h$ of the hole component of the exciton is constant with temperature at a value[19] $E_h = 35$ meV ($E_x = E_t + E_h$), then these data indicate a reduction in the Cd-O electron binding energy of $\approx 30$ meV as the temperature is raised from 10 to 300 °K.

### C. Zinc-Oxygen Impurity Complex

Luminescence excitation spectra for recombination at Zn-O nearest-neighbor complexes have been reported previously for several temperatures by Welber and Morgan.[31] We have obtained essentially similar results from the crystal used for the oxygen luminescence excitation data in Fig. 3. Some representative spectra are shown in Fig. 9. As in the case of the O and Cd-O excitation spectra, three prominent features are observed. The peak of the Zn-O absorption band occurs at $A$, absorption due to nitrogen isoelectronic centers is observed at $B$, and at $C$ we find luminescence excitation due to capture of photogenerated electrons onto the Zn-O complexes. In contrast to the results of Welber and Morgan,[31] we do not find, for the crystal described in Fig. 9, excitation of the red luminescence through absorption at nitrogen centers at the lowest temperatures. (This was also noted to be the case for the Cd-O excitation spectra studied in Fig. 6.) In the same crystal, however, we do find excitation of the infrared oxygen luminescence due to absorption at nitrogen centers even at 1.8 °K as shown in Fig. 3. To explain the excitation of the red luminescence by nitrogen absorption at 7 °K in the crystal which they studied, Welber and Morgan suggested a resonant transfer of energy from an exciton bound at a nitrogen center to an excited state of the exciton bound to the Zn-O complex. The excited state of the exciton presumably decays rapidly to the ground state, and then recombines to emit the red luminescence. The rate of resonant transfer of energy in this model depends on the product of concentrations of Zn-O and N centers. In the crystal which we investigated (Figs. 3 and 9), the Zn-O concentration is low (probably less than $10^{15}$ cm$^{-3}$) as compared with that of oxygen ($\sim 10^{17}$ cm$^{-3}$).

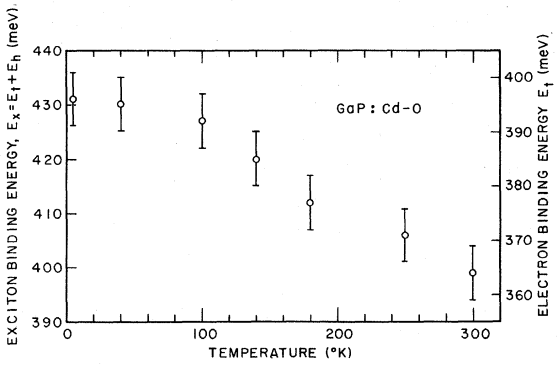


FIG. 8. Temperature variations of exciton binding energy $E_x$ and the electron binding energy $E_t$ of the Cd-O complex obtained from the temperature dependence of the peak absorption energy $E_{ab}$ using Eq. (13). Energy $E_t = E_x - E_h$ has been calculated assuming $E_h = 35$ meV over the entire temperature range.

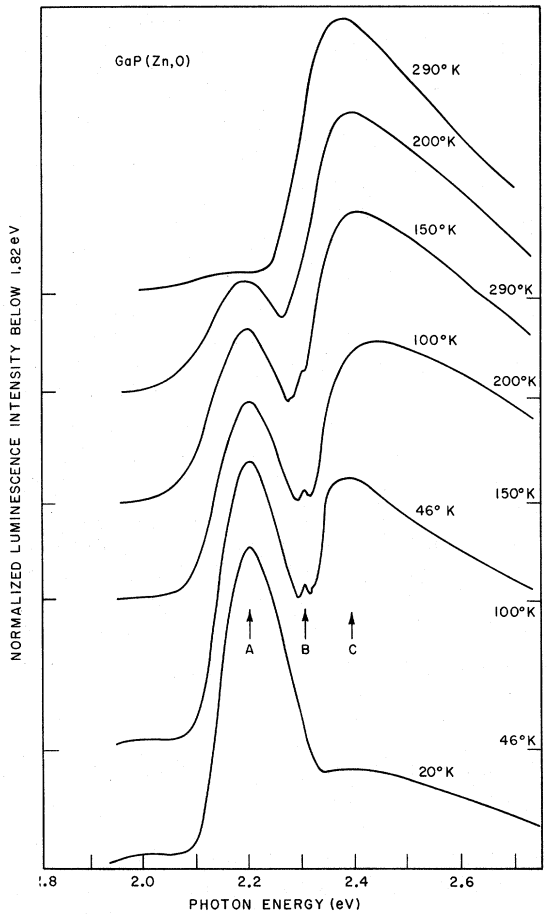


FIG. 9. Photoluminescence excitation spectra of the neutral Zn-O impurity complex at several temperatures obtained by monitoring the red luminescence between 1.82 and 1.44 eV. The zero levels have been shifted as in Fig. 3. Structure at $A$, $B$, and $C$ is discussed in the text.

Thus, resonant transfer or tunneling of the exciton from N to O centers is more likely to occur in our sample than transfer from N to Zn-O centers.

In Fig. 10 we plot the effective width $W$ for the Zn-O absorption band versus temperature. Again we find that the single-linear-mode model fits the data with $\hbar\omega = 18.8$ meV [see Eq. (10)]. If we assume that the ratio $W/W_A$ is the same for the Zn-O band as for the Cd-O band, then we can find the constant $a$ for the Zn-O absorption by comparing the low-temperature widths of the Cd-O and Zn-O bands using Eq. (10). When this is done we obtain $a = 3.87$. This gives a value of $\frac{1}{2}a^2\hbar\omega$ in Eq. (13) which is only 2 meV larger for Zn-O than Cd-O. We can use Eq. (13) to solve for $E_x$ and $E_t$ as a function of temperature as we did for the Cd-O absorption. Here we take[19] $E_h = 36$ meV for the binding energy of the hole component of the exciton bound to the Zn-O site. The results are plotted in

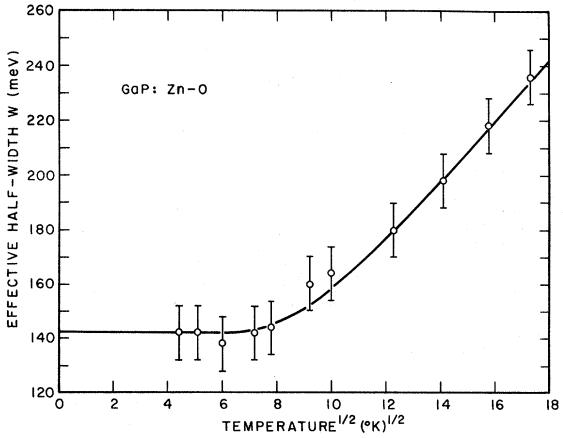


FIG. 10. Effective half-width $W$ for the Zn-O absorption band as a function of the square root of temperature. Solid curve is fit of Eq. (10) to the data obtained by taking $\hbar\omega = 18.8$ meV.

Fig. 11. These calculations predict that the Zn-O trap depth is reduced from 266 meV at 10 °K to a value of 220 meV at room temperature. Independent room-temperature determinations[8,21] of $E_t$ from thermal quenching of the red luminescence yield $E_t = 230 - 240$ meV, in reasonable agreement with the value obtained here.[32]

## IV. ABSORPTION DUE TO INADVERTENTLY PRESENT IMPURITIES

We show in Fig. 12 room-temperature absorption spectra[33] obtained from transmission measurements for Zn, O-doped crystals. Figure 12(a) gives the complete absorption spectrum showing both the high-energy tail ($h\nu < 1$ eV) of the infrared

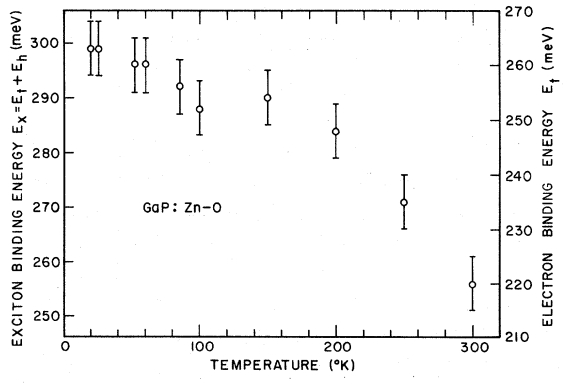


FIG. 11. Temperature variations of the exciton binding energy $E_x$ and the electron binding energy $E_t$ of the Zn-O complex obtained from the temperature dependence of the peak absorption energy $E_{ab}$ using Eq. (13). Energy $E_t = E_x - E_h$ has been calculated assuming $E_h = 36$ meV over the entire temperature range.

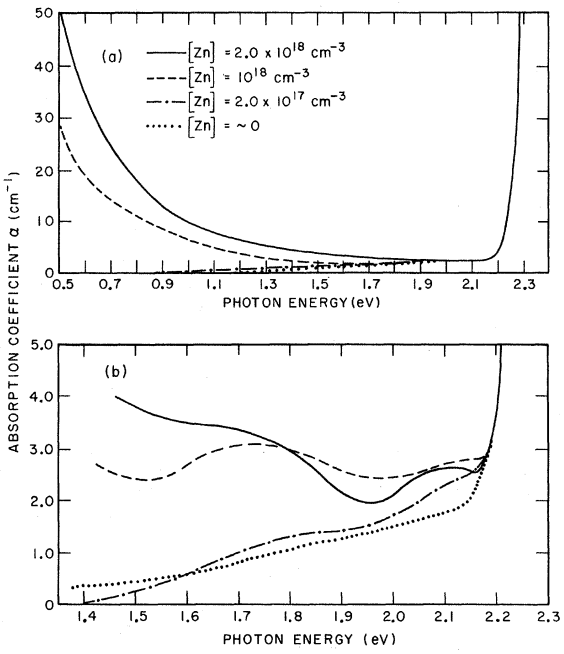


FIG. 12. Absorption spectra obtained from transmission measurements at 300 °K for GaP crystals containing $[O] \approx 10^{17}$ cm$^{-3}$ and four different concentrations of Zn. (a) Spectra in the range 0.5 eV $< h\nu <$ 2.3 eV showing differences in feee-carrier absorption for crystals heavily and lightly doped with Zn. (b) Detailed spectra below the band gap showing absorption bands due to neutral oxygen (at 1.75 eV) and the Zn-O complex (at 2.1 eV).

free-carrier absorption[7] and the onset of the indirect edge[1-4] for $h\nu > 2.2$ eV. In the region between 1.4 and 2.2 eV the absorption is small, typically < 5 cm$^{-1}$. However, as shown in Fig. 12(b), considerable structure is observed in this energy range. The most prominent feature of the absorption is the broad band at ≈1.75 eV in the crystal doped with a Zn-acceptor concentration of $10^{18}$ cm$^{-3}$. Also evident is the band at ≈2.1 eV. We conclude by comparing the positions and shapes of these bands with the photoluminescence excitation absorption spectra of Figs. 3 and 9 and find that they are due to isolated O donors and nearest-neighbor Zn-O complexes. The data in Fig. 12(b) show rather clearly that the weakly Zn-doped crystals and the undoped crystal have absorption spectra near the band edge which are very similar to the spectra of the more heavily Zn-doped crystals. We propose that the similarities in these spectra can be understood by considering the influence of inadvertently added impurities to the solution grown crystals.

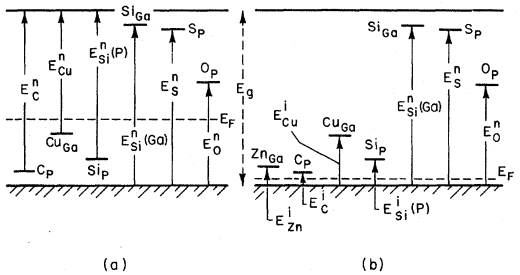


FIG. 13. Schematic energy level diagram for GaP showing energy levels and optical transitions associated with probable inadvertently present donors and acceptors. Subscripts on labels for donors and acceptors indicate whether they are situated on a Ga or P site. Notation associated with optical transitions are as in Table I. (a) Weakly $p$-type crystals with the Fermi-level $E_F$ near the center of the gap. (b) More heavily $p$-type crystals with Fermi level near the Zn acceptor.

TABLE I. Impurity absorption threshold transition energies at 300 °K and donor-acceptor binding energies in GaP ($E_g$ = 2.26 eV).

| Impurity[a] | Binding energy (eV) | Threshold transition energy[b] (eV) |
|---|---|---|
| $C_P(A)$ | 0.048[c] | $E_C^n = 2.21$<br>$E_C^i = 0.0475$ |
| $Cu_{Ga}(A)$ | 0.6–0.7[d] | $E_{Cu}^n = 1.56$–$1.66$<br>$E_{Cu}^i = 0.6$–$0.7$ |
| $Si_P(A)$ | 0.204[c] | $E_{Si}^n(P) = 2.16$<br>$E_{Si}^i(P) = 0.2$ |
| $Si_{Ga}(D)$ | 0.08[c] | $E_{Si}^n(Ga) = 2.18$ |
| $S_P(D)$ | 0.102[c] | $E_S^n = 2.16$ |
| $O_P(D)$ | 0.90 | $E_O^n = 1.4$ |

[a]We designate whether an impurity is a donor or acceptor by $D$ and $A$, respectively.

[b]The notation $E^n$ and $E^i$ refers, respectively, to photo-neutralizing and photo-ionizing transitions.

[c]Reference 35.

[d]Reference 36.

Solution-grown GaP crystals have been shown[34,35] to contain a number of donor-acceptor impurities, some of which are indicated schematically in Fig. 13 for what is thought to be two likely situations. Figure 13(a) applies to a nominally undoped crystal (weakly $p$ type) while Fig. 13(b) applies to a Zn-doped crystal. In either case oxygen is thought to enter the crystal via a reaction with walls of the quartz ampoules. Since the crystals are $p$ type, the Fermi level $E_F$ falls below the O level and so photoneutralizing transitions to oxygen should always be present (threshold ~1.4 eV at 300 °K). These are indicated by $E_O^n$ in Figs. 13(a) and 13(b). Other common impurities are Si, S, and C.[35] Evidence has also been presented[36] for the presence of deep Cu acceptors in GaP. We have schematically indicated all of these impurities in Fig. 13

and have labeled the sublattice on which they appear by the subscripts Ga and P. Depending on the position of the Fermi level, different types of transitions are possible. Because the crystals are $p$ type, the donors participate in photoneutralization absorption indicated by $E^n$. The acceptors can contribute either to photoneutralization absorption in weakly $p$-type crystals [Fig. 13(a)] or to photo-ionization absorption ($E^i$) in heavily $p$-type crystals [Fig. 13(b)]. Table I summarizes the threshold transition energies expected for the various impurities at room temperature. It is important to note that the spectral shapes of the impurity absorption bands are sensitive not only to whether a given absorption process is photoneutralization or photo-ionization, but also to the depth of the impurity level and the strength of coupling of the impurity to the lattice. Based on the considerations leading to Eq. (8) we conclude that the photoneutralization transitions shown in Fig. 13 and listed in Table I should give rise to broad absorption bands which overlap the indirect edge considerably. We also conclude, based on Bebb's analysis,[15] that the photo-ionization transitions from the deeper acceptors (Si, Cu) should give a large background absorption which extends to energies ~10 times the acceptor ionization energy. We now incorporate these ideas into our interpretation of the data given in Fig. 12.

We may reasonably expect that the various inadvertent impurities in $p$-GaP will give a low-energy absorption tail on the band edge due to photoneutralization of both donors and acceptors, and a high-energy tail extending into the visible on the infrared free-carrier absorption due to photoionization of acceptors. In Fig. 14 we compare the absorption from an O-doped crystal [Fig. 14(a)] with one doped with O and Zn [Fig. 14(b)] (Zn concentration $\approx 2\times10^{17}$ cm$^{-3}$). The data in Fig. 14(a) indicate that the room-temperature threshold absorption is $h\nu \approx 1.4$ eV, in agreement with the O threshold absorption in Fig. 3. We suggest that the absorption at 300 °K in Fig. 14(a) is due to the photoneutralizing transitions in Fig. 13(a) and that the smooth increase in absorption with increasing photon energy is due principally to successive absorptions from O, Cu,[37] and Si. The 80 °K absorption spectrum is consistent with this interpretation. Since the crystal is weakly $p$ type, the room-temperature Fermi level $E_F$ will lie below midgap between the deepest acceptor and deepest donor, with the donors preferentially compensating the deeper acceptors. At lower temperatures the holes will freeze out on the deep acceptors and the donors will preferentially compensate the shallower acceptors with the result that $E_F$ will move toward the shallow acceptor levels. Thus, at 80 °K, we expect $E_F$ to lie near the Si or C acceptor levels in

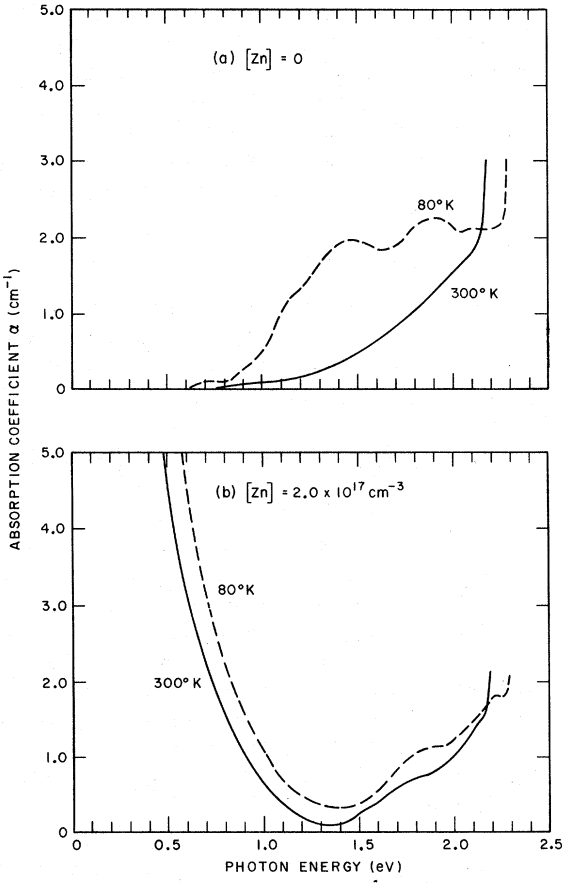


FIG. 14. Absorption spectra showing differences at 300 and 80 °K of crystals (a) doped only with oxygen, and (b) lightly doped with zinc and oxygen.

Fig. 13(a), and, as a consequence, the photo-ionization absorption of Cu should become dominant. The 80 °K data in Fig. 14(a) have a threshold at $h\nu \approx 0.8$ eV and reach a broad maximum at $\approx 1.5$ eV. These data appear to be consistent with the presence of Cu acceptors (see Table I).[37] Above $h\nu \approx 1.5$ eV the O absorption superimposes on the Cu photoionization absorption giving rise to a broad absorption background below the indirect edge.

In Fig. 14(b), the data for a crystal containing $\approx 2\times10^{17}$ cm$^{-3}$ Zn acceptors are consistent with this interpretation. The 300 and 80 °K spectra are very similar. As indicated in Fig. 13(b) the Fermi level for this situation is controlled by the Zn. The infrared absorption for $h\nu < 1$ eV is due to free carriers at 300 °K and photo-ionization from Zn at 80 °K.[7] The spectrum for $h\nu > 1.5$ eV is due to the photoneutralization processes discussed above. Because the Cu photo-ionization absorption is absent in Fig. 14(b) we may conclude, on the basis of our model, that the Cu contamination varies substantially in different crystals.[37] Finally, we note that

for all Zn-doped crystals examined, the absorption spectra in the range $0.6\text{ eV} < h\nu < 1.2\text{ eV}$ could fit approximately through the relation $\ln[\alpha(h\nu)] \propto -h\nu/kT$. This behavior can be understood either on the basis of inter-valence-band absorption,[7] or as the high-energy tail of photoneutralization or photo-ionization absorptions by impurities strongly coupled to the lattice.

## V. ABSORPTION AND EMISSION RATES

It has been customary to determine the concentrations of impurities in semiconductors through the use of the well-known "Smakula's equation," given in a generalized form by[16]

$$Nf_{ab} = \frac{m^*c}{2\pi^2 e^2 \hbar}\, n(E_{ab}) \left[\frac{\xi_0}{\xi_{eff}(E_{ab})}\right]^2 \int \alpha(E)\, dE\,. \tag{14}$$

In this equation $N$ is the concentration of impurities, $f_{ab}$ is the oscillator strength of the absorption process between states $a$ and $b$, $\alpha(E)$ is the absorption coefficient, $E_{ab}$ is the energy position of the maximum of the absorption band, and $m^*$ is the effective mass. [The other constants have been previously defined in Eq. (2).] It is usually assumed that the oscillator strength is related to the radiative lifetime $\tau_{ba}$ of the inverse luminescent process through the relation[16]

$$f_{ab} = \left(\frac{\hbar^2 c^3 m^*}{2e^2}\right) \frac{1}{n(E_{ba})} \left(\frac{\xi_0}{\xi_{eff}(E_{ba})}\right)^2 \left(\frac{1}{E_{ba}^2}\right)\left(\frac{1}{\tau_{ba}}\right), \tag{15}$$

where $E_{ba}$ is the position of the maximum of the luminescent band. Fowler and Dexter[17] have shown that in general, Eq. (15) does not hold in a solid. They find that it should be replaced by a more general expression:

$$f_{ab} = \left(\frac{\hbar^2 c^3 m^*}{2e^2}\right) \frac{1}{n(E_{ba})} \left(\frac{\xi_0}{\xi_{eff}(E_{ba})}\right)^2 \times \frac{E_{ab}}{E_{ba}^3} \frac{|M_{ab}|^2}{|M_{ba}|^2} \frac{2J_b+1}{2J_a+1} \left(\frac{1}{\tau_{ba}}\right), \tag{16}$$

where $M_{ab}$ and $M_{ba}$ are the dipole matrix elements for the absorption and emission processes, respectively, and $J_a$ and $J_b$ are the angular momentum quantum numbers for the lower and upper states, respectively. Equation (16) differs from Eq. (15) primarily through the ratio of the squared matrix elements. We expect this ratio to deviate from unity in the case where the configuration of the lattice differs greatly between the emission and absorption processes, i.e., if there is a large Stokes shift.

As we have seen, there is a large Stokes shift ($\approx 360$ meV) between absorption and emission at Zn-O. Hence, we expect that it will be mandatory to use Eq. (16) for this center. In a previous study,[8] we have determined the concentrations of Zn-O centers in several crystals of $p$-GaP independently of Smakula's equation by means of five photoluminescence measurements. We now use these results to determine the ratio $R$, defined by

$$R = \left(\frac{\xi_{eff}(E_{ba})}{\xi_{eff}(E_{ab})}\right)^2 \frac{2J_a+1}{2J_b+1} \frac{|M_{ba}|^2}{|M_{ab}|^2}\,. \tag{17}$$

Combining Eqs. (14), (16), and (17) we obtain

$$N = (4.25\times 10^{23})\, Rn(E_{ab})n(E_{ba})(E_{ba}^3/E_{ab})\,\alpha_0 \Delta E \tau_{ba}\,, \tag{18}$$

where we have assumed that the absorption band is Gaussian with a maximum value $\alpha_0$ and a half-width $\Delta E$. For Zn-O the values of the constants entering Eq. (18) are $n(E_{ab}) = 3.46$, $n(E_{ba}) = 3.33$, $E_{ba} = 1.77$ eV, $E_{ab} = 2.13$ eV, and $\Delta E \cong 0.24$ eV. Including screening effects (for a crystal with hole concentration $\sim 10^{18}$ cm$^{-3}$) $\tau_{ba} = 2\times 10^{-7}$ sec for the radiative Zn-O lifetime.[8] In a crystal in which $\alpha_0 = 1.3$ cm$^{-1}$, we find $N = 2.9\times 10^{16}$ cm$^{-3}$. Hence,

$$R(\text{Zn-O}) = 0.37\,.$$

For the O centers, at which the absorption and emission processes involve a continuum of valence-band states, Eq. (18) is no longer directly applicable. Blakemore[38] has shown in this case that the radiative lifetime $\tau_r$ of the emission is related to the absorption photo-cross-section $\sigma_b$ [Eq. (4)] by

$$\frac{1}{\tau_r} = \frac{g_d n^2}{\pi^2 \hbar^3 c^2} \int_0^\infty E^2 \sigma_b(E) f_v(E_v)\, dE_v\,, \tag{19}$$

where $E$ is the photon energy, $f_v$ is the occupation factor for holes in the valence band, $g_d$ is the statistical weight of the O donor, and the integral is taken over the valence-band energy $E_v$. We may evaluate the integral in Eq. (19) approximately by noting that the product $E^2\sigma_b(E)$ is practically constant with $E = E_{ab}$ over the range of $E_v$ for which the factor $f_v$ is nonvanishing. Taking this product outside the integral, and writing the Fermi factor as $f_v = (p/N_v)e^{-E_v/kT}$, Eq. (19) becomes

$$\frac{1}{\tau_r} = \frac{g_d n^2}{\pi^2 \hbar^3 c^2}\, E_{ab}^2 \sigma(E_{ab}) \frac{p}{N_v} kT\,, \tag{20}$$

where $p$ is the free hole density and $N_v$ is the valence-band effective density of states. In a previous study[8] of a crystal in which $p = 1.2\times 10^{18}$ cm$^{-3}$ at 300 °K, we found $\sigma_b(E_{ab}) = 4\times 10^{-18}$ cm$^2$ and $25 \leq \tau_r \leq 76$ $\mu$sec. Evaluating Eq. (20) for this value of $p$ and using $N_v = 1.8\times 10^{19}$ cm$^{-3}$, we obtain $\tau_r = 6$ $\mu$sec. Since the lifetime calculated from the experimental photo-cross-section is shorter than the measured lifetime, we again find that the lattice coupling enhances absorption relative

to emission, i.e.,

$$0.08 \leq R(\text{oxygen}) \leq 0.25 \ .$$

## VI. SUMMARY AND CONCLUSIONS

We have presented detailed data showing the temperature dependence of the optical absorption bands due to the deep oxygen donor and the Cd-O and Zn-O isoelectronic centers in $p$-GaP. We have found that the Cd-O and Zn-O bands can be described by a simple classical model in which the impurities are coupled to a single linear lattice-vibrational mode. Utilizing this model we have found that the electron binding energy of the Cd-O isoelectronic complex decreases from 396 to 364 meV over the temperature range 10–300 °K. Over the same range the electron binding energy of the Zn-O center decreases from 260 to 220 meV. The applicability of the semiclassical model to these centers indicates that their absorption properties are dominated by exciton transitions.

For the oxygen donor, exciton effects are apparently absent. Both coupling to the lattice as well as the continuum nature of the initial electronic states of the optical transition contribute to the shape of the absorption spectrum. We find that the oxygen absorption band can be described qualitatively by combining the usual (effective-mass) band-to-impurity model for impurity absorption in direct-gap compounds with the configuration-coordinate approach which accounts for the lattice coupling.

Because of lattice coupling, the oscillator strengths of the emission and absorption processes (even the no-phonon processes) can differ significantly. For both O and Zn-O, we have found that the oscillator strength for absorption is enhanced relative to the oscillator strength for the inverse emission process.

Finally, we have noted that the optical absorption spectra of zinc- and oxygen-doped $p$-GaP are to a large degree dominated by the individual absorption bands due to O and Zn-O centers. In addition, significant absorption contributions are observed due to inadvertently present donors and acceptors. These inadvertent impurities produce absorption tails both on the low-energy side of the band edge, and on the high-energy side of the free-carrier absorption spectrum.

## ACKNOWLEDGMENTS

We wish to thank F. A. Trumbore and L. Derick for providing the crystals used in this study, and R. H. Saul for assistance in determining the effect of surface preparation on the absorption coefficient. It is a pleasure to acknowledge the assistance of E. F. Kankowski and M. L. Howe in the experimental work.

[1]P. J. Dean and D. G. Thomas, Phys. Rev. 150, 690 (1966), and references cited therein.

[2]P. J. Dean, G. Kaminsky, and R. B. Zetterstrom, J. Appl. Phys. 38, 3551 (1967).

[3]M. R. Lorenz, C. D. Pettit, and R. C. Taylor, Phys. Rev. 171, 876 (1968).

[4]M. B. Panish and H. C. Casey, Jr., J. Appl. Phys. 40, 163 (1969).

[5]W. O. Spitzer, M. Gershenzon, C. J. Frosch, and D. F. Gibbs, J. Phys. Chem. Solids 11, 339 (1959).

[6]J. D. Wiley and M. DiDomenico, Jr., Phys. Rev. B 1, 1655 (1970).

[7]J. D. Wiley and M. DiDomenico, Jr., Phys. Rev. B 3, 375 (1971).

[8]J. M. Dishman, M. DiDomenico, Jr., and R. Caruso, Phys. Rev. B 2, 1988 (1970).

[9]T. Mizanchi, H. Sonomura, and N. Yamamoto, Japan. J. Appl. Phys. 8, 886 (1969).

[10]P. J. Dean and C. H. Henry, Phys. Rev. 176, 928 (1968).

[11]P. J. Dean, C. H. Henry, and C. J. Frosch, Phys. Rev. 168, 812 (1968).

[12]J. M. Dishman, Phys. Rev. B 3, 2588 (1971).

[13]D. M. Eagles, J. Phys. Chem. Solids 16, 76 (1960).

[14]W. P. Dumke, Phys. Rev. 132, 1998 (1963).

[15]H. B. Bebb, Phys. Rev. 185, 1116 (1969).

[16]See, for example, the review article by D. L. Dexter, in *Solid State Physics*, edited by F. Seitz and D. Turnbull (Academic, New York, 1958), Vol. 6.

[17]W. B. Fowler and D. L. Dexter, Phys. Rev. 128, 2154 (1962).

[18]T. N. Morgan, B. Welber, and R. N. Bhargava, Phys. Rev. 166, 751 (1968).

[19]C. H. Henry, P. J. Dean, and J. D. Cuthbert, Phys. Rev. 166, 754 (1968).

[20]C. H. Henry, P. J. Dean, D. O. Thomas, and J. J. Hopfield, in *Proceedings of the Conference on Localized Excitations*, edited by R. F. Wallis (Plenum, New York, 1968), p. 267.

[21]J. S. Jayson, R. N. Bharagava, and R. W. Dixon, J. Appl. Phys. 41, 4972 (1970).

[22]H. Welker, J. Electron. 1, 181 (1955).

[23]For example, see J. F. Miller, in *Compound Semiconductors*, edited by R. K. Willardson and H. L. Goering (Reinhold, New York, 1962), Vol. 1, Chap. 23.

[24]These values were obtained from surface barrier capacitance data kindly provided by W. H. Hackett, Jr.

[25]H. Reiss, C. S. Fuller, and F. J. Morin, Bell System Tech. J. 35, 535 (1956).

[26]J. D. Wiley, J. Phys. Chem. Solids (to be published).

[27]J. M. Dishman and M. DiDomenico, Jr., Phys. Rev. B 1, 3381 (1970); in *Proceedings of the International Conference on the Physics of Semiconductors, Cambridge*, 1970 (U. S. Atomic Energy Commission, Oak Ridge, Tenn., 1971), p. 607.

[28]R. A. Faulkner, Phys. Rev. 184, 713 (1969).

[29]J. M. Dishman (unpublished).

[30]See, for example, the most recent quantum formulation of the configuration-coordinate model by T. H. Keil, Phys. Rev. 140, A601 (1965), and the references to earlier work found therein.

[31]B. Welber and T. N. Morgan, Phys. Rev. 170, 767

(1968).

[32]Our result differs somewhat from that found by other investigators. Thus, J. D. Cuthbert, C. H. Henry, and P. J. Dean [Phys. Rev. 170, 739 (1968)] estimated $E_t = 300$ meV at 4 °K by assuming the no-phonon energy $E_{np}$ to be the mean of the absorption and emission peak energies. A. Kasami, Japan. J. Appl. Phys. 9, 946 (1970), finds 289 eV $\leq E_t \leq$ 310 meV at 300 °K from his data on the temperature dependence of the photocurrent and decay time in red diodes of GaP (Zn, O).

[33]Absorption spectra of Zn, O-doped crystals grown by the liquid encapsulation technique have been recently reported by S. D. Lacey, Solid State Commun. 8, 1115 (1970). Although his data are qualitatively similar to those reported here, his values for $\alpha$ are somewhat higher than ours on crystals of similar doping level.

[34]D. G. Thomas, M. Gershenzon, and F. A. Trumbore, Phys. Rev. 133, A269 (1964).

[35]P. J. Dean, C. J. Frosch, and C. H. Henry, J. Appl. Phys. 39, 5631 (1968).

[36]J. W. Allen and R. J. Cherry, J. Phys. Chem. Solids 23, 509 (1962); B. Goldstein and S. S. Perlman, Phys. Rev. 148, 715 (1966).

[37]We make this identification of Cu somewhat advisedly, since recent work [J. M. Dishman, D. F. Daly, Jr., and W. P. Knox (unpublished)] has shown the existence of at least one other $\sim 0.7$-eV acceptorlike level which is probably due to a native lattice defect.

[38]J. S. Blakemore, Phys. Rev. 163, 809 (1967).